# Estimating the stresses within the lithosphere: parameter check with applications to the African Plate

© *S. Medvedev[1] and "The African Plate" Working group[1,2], 2010*

[1]Physics of Geological Processes, Oslo University, Oslo, Norway
sergeim@fys.uio.no
[2]Center for Geodynamics, NGU, Trondheim, Norway

Several mechanisms control the state of stress within plates on Earth. The list is rather long, but well known and includes ridge push, mantle drag, stresses invoked by lateral variations of lithospheric density structure and subduction processes. We attempt to quantify the influence of these mechanisms and to construct a reliable model to understand modern and palaeo-stresses using the African plate (TAP) as an example.

Constructing the base model lithosphere of TAP we follow [Steinberger et al., 2001]. Combining data on topography, age of ocean floor and global model for crust structure, CRUST2 [Bassin et al., 2000], we compute the gravitational potential energy (GPE) for the entire TAP. GPE, proportional to the double integration of the density profile through thickness of the model lithosphere, describes the forces rising from lateral density heterogeneities within lithosphere. In particular, GPE of the base model accounts for push from the mid-oceanic ridges surrounding TAP and stresses rising from the crustal thickness changes.

The finite-element based suite ProShell was utilized to calculate stresses using the real, non-planar geometry of TAP. The modeled results are tested and iterated to match the observed stress pattern recorded or derived from observations. We combined several studies to complete set of observational data. That includes non-seismic data from WSM [Heidbach et al., 2008], compilation of the field observation [Bird et al., 2006], and integrated inversion of focal mechanism data [Delvaux, Barth, 2010]. Fig. 1 presents the distribution of data on stress regimes and orientation of most compressive mean stress. We adopted several numerical characteristics describing proximity of model results and observations: 1) the average misfit angle is the mean difference in orientations; 2) the angle fitting factor is the percentage of the number of observa-

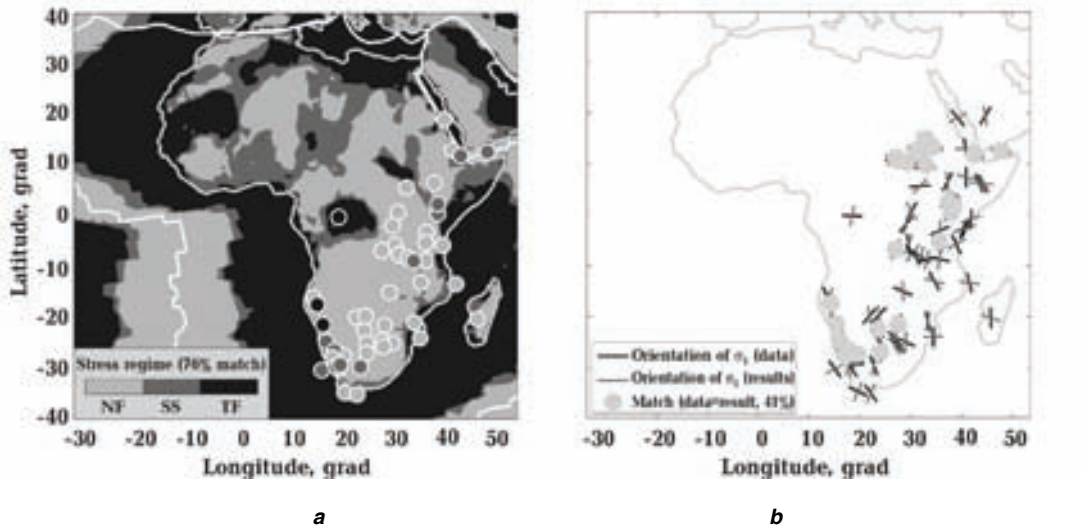


Fig. 1. Results for model 3 represents typical distribution of the stress regimes with TAP (*a*) and orientation of maximal compressive stresses (marked as $\sigma_1$ on the (*b*) panel). The results of the model are compared to observations (see text for description of data). The data represented by markers on the (*a*). Green discs cover the results with orientation within 90 % confidence interval of observations on the (*b*) panel.

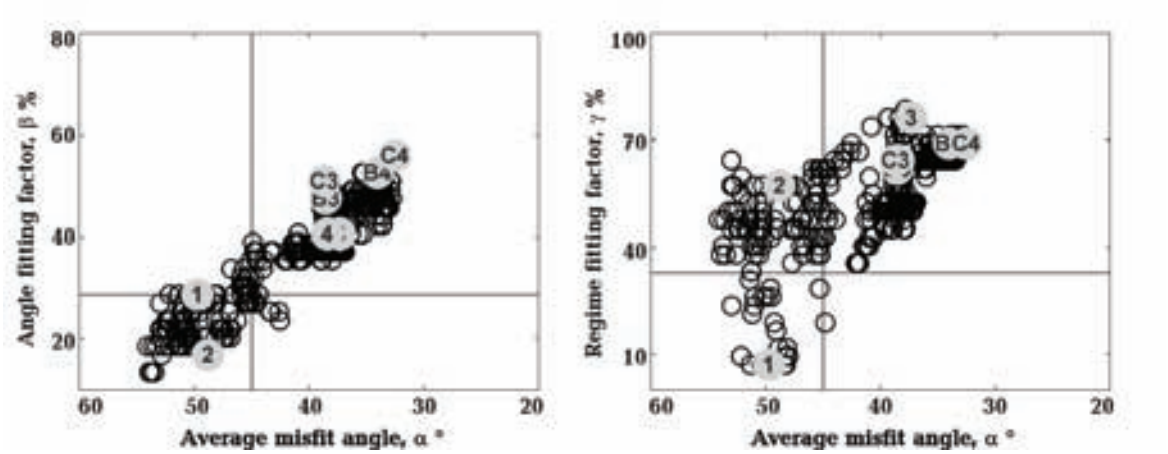


Fig. 2. Illustration of variation of fitting parameters for different sets
different sets of parameters variations, circles filled with green represent successful representatives of each set (marker 4 covers marker for model 3 on (*a*), marker C3 covers B3 and marker C4 covers C3 on (*b*) panel). See text for description of the numerical experiments series and definitions of fitting parameters. Blue lines present random average values, the results that follow below or (*a*) from these lines represent light autocorrelation with observations.

tions which fits to model results within 90 % confidence interval of the data; 3) regime fitting factor is the percentage of the successful match of observed and modeled regimes.

Fig. 2 presents the fitting characteristics for approximately 700 model runs. The figure also shows that the results may fall below limit provided by random average. The results of base model (Fig. 2, model 1) compares poorly with observations. This model presents the simplest combination of simple models and widely available data and it assumes that the top of the mantle lithosphere (Moho) has constant temperature, which is clear oversimplification for model of TAP, which includes mid-oceanic ridges and thick continents. The model 2 (Fig. 2) assumes that the Moho temperature is proportional to the thickness of the crust above. This model, however, does not show significant improvement while compared to model 1 for variety of the coefficients of proportionality between crustal thickness and Moho temperature, $\Delta T$.

Two previous models are based on the prescribed thickness of the crust (given by CRUST2) and model topography does not match exactly the observed topography of TAP. In model 3 we assume that the CRUST2 model is inaccurate. We stretched the thickness of the model crust so that after isostatical adjustment observed and model topography match exactly. Varying $\Delta T$ within model 3 we found that the optimal value for constant $\Delta T$ within TAP and improve significantly the match between model results and observation.

The density of mantle within models 1—3 depends only on thermal state of mantle, which in turn depends on the age and crustal thickness. The observations, however, point out existence of significant compositional (and thus, density) variations of the mantle beneath TAP. In model 4 we assume that part of mismatch between CRUST2 — based topography and observed topography is associated mantle density variations. That was emulated by variations of effective thermal situation, simply by assuming $\Delta T$ varies laterally.

In addition to the stresses directly resulted from GPE, we considered several additional complications of the model. In series B we considered basal drag caused by sub-mantle flow derived from mantle convection model. We couple this flow filed to models 3 and and vary parameters of coupling. Whereas the model B3 shows little improvement compared to model 3, the basal drag with reasonable parameters of coupling improves significantly model with variable density of the lithospheric mantle (model 4 vs, model B4).

All the models considered above are based on uniform rheological properties of TAP. This is very strong simplifying assumption. In model series C we considered simplest variations of rheological properties, assigning weakening along mid-oceanic ridges. The results improve (model C4) when weakening related to young age of the ocean floor is by up to two orders of magnitude.

## References

*Bassin C., Laske G., Masters G.* The Current Limits of Resolution for Surface Wave Tomography in North America // EOS Trans AGU. — 2000. — **81**. — P. F897.

*Bird P., Ben-Avraham Z., Schubert G., Andreoli M., Viola G.* Patterns of stress and strain rate in southern Africa // J. Geophys. Res. Sol. Earth. — 2006. — **111**. — P. Bo8402. — DOI:10.1029/2005JB003882.

*Delvaux D., Barth A.* African stress pattern from formal inversion of focal mechanism data // Tectonophysics. — 2010. — **482**. — P. 105—128.

*Steinberger B., Schmeling H., Marquart G.* Large-scale lithospheric stress field and topography induced by global mantle circulation // Earth Planet. Sci. Lett. — 2001. — **186**. — P. 75—91.